



# Ceramic-metal interface: Effect of titanium activity on interfacial microstructure formation in vacuum-brazed Al<sub>2</sub>O<sub>3</sub>/Al alloy joints

Sundara Dhas Stalin<sup>®</sup>\*, Kani Kalaichelvan

Department of Ceramic Technology, Alagappa College of Technology Campus, Anna University, Chennai - 600 025, Tamil Nadu, India

Received 5 February 2025; Received in revised form 25 August 2025; Accepted 7 September 2025

#### Abstract

Plasma-assisted physical vapour deposition of titanium over an alumina surface, brazed with an aluminium alloy substrate using Al4047 filler, was conducted in a vacuum ranging from  $1\times10^{-3}$  to  $10^{-5}$  mbar. Microstructure characterization, specifically focusing on the  $Al_2O_3$ -Ti coating interface, aims to explain what mechanism underlies the secure bonding of ceramics to metal and how vapour deposition and vacuum atmosphere play a crucial role in achieving this feasibility. Titanium enhanced the wetting characteristics of the alumina surface through chemical reactions. The  $TiO_2$  and  $Ti_3Al$  reaction compounds were identified at the interface. The Ti-rich phase adjacent to the  $Al_2O_3$  substrate becomes increasingly discontinuous with brazing time. At the  $Al_2O_3$ -Ti interface, a reaction layer of 0.5-1  $\mu$ m thickness was observed at a brazing temperature of 582 °C held for 40 min. In demonstrating defect-free, solidly packed joints, the proposed additive manufacturing approach affirms its suitability for fabricating  $Al_2O_3$ -Al composites at lower joining temperatures, based on the effect of titanium on interfacial bonding characteristics.

**Keywords:** Al<sub>2</sub>O<sub>3</sub>/Ti interfaces, vapour deposition, brazing, composites

# I. Introduction

Vacuum brazing is a prominent joining technology for fabricating ceramic-metal composites that integrates alumina (Al<sub>2</sub>O<sub>3</sub>) with aluminium alloy and has expanded its prospects, predominantly in sensor feedthroughs. This joining technology is extensively integrated into ultra-high vacuum modules, which support manifold requirements in electronics, biomedical applications and the chemical equipment [1–5]. Hermetic biocompatible packaging necessitates implantable devices, such as electromagnetic interference (EMI) feedthrough filters for cardiac pacemakers and defibrillators, spinal cord stimulators (SCS) and implantable MyoElectric sensors (IMES) for prosthetic control systems. Implanted biomedical microsystems consist of application specific integrated circuits (ASICs) encapsulated in biocompatible materials, featuring various electrical feedthroughs linked to stimulation [6–8]. Desirable characteristics of implantable electrical devices include long-term stability, extreme

miniaturization, hermetic sealing, and biocompatibility [5,9,10]. The substantial impact on joining ceram-

ics was because of their essential properties, with ex-

cellent chemical permanence, strong resistance to de-

formation, a high dielectric influence, improved ther-

mal stability and abrasiveness in hostile environments

[11]. Challenges of alumina brazing are poor wettability

and high residual stress at ceramic-metal interface be-

cause of the variation in thermal expansion coefficients

[12]. In the realm of advanced joining technologies, a

variety of bonding methods have surfaced for the pur-

pose of joining metal alloys with ceramics. The methods

encompass diffusion bonding, active brazing, transient

liquid-phase bonding and ultrasonic welding [13,14].

Active metal brazing is the most preferred method for ceramic joining applications among these cutting-edge joining methods.

The initiation of an interfacial reaction via brazing is required to secure strong joints. When the active metal element is introduced to the filler alloy, it initiates a chemical reaction at the ceramic-metal interface. It facilitates the adequate bonding of ceramics and reduces interfacial residual stress formation. Ti, V, Nb, Hf, Ta

<sup>\*</sup>Corresponding authors: tel: +91 9894392109, e-mail: *stalingodson@yahoo.com* 

and Zr are some of the active metals in the IV and V groups of the Periodic table. They can modulate the ceramic substrate to be hydrophilic and substantially subjected to its interfacial chemistry [15-18]. For example, through the chemical reaction of molten Ag-Cu-Ti filler with Al<sub>2</sub>O<sub>3</sub>, the wettability of the monocrystalline alumina surface improved as the contact angle decreased to 10° with the addition of titanium content (3 and 8%) [19]. The formation of chemically reacted compounds was characterized by a continuous reaction layer of micrometre size at the interface [20,21]. Two distinct intermetallic compound layers are formed with Ti-O and Ti-Cu-O phases at the interfaces where the Al<sub>2</sub>O<sub>3</sub> ceramic-active metallic (Ag-Cu-Ti) filler is. So far, the observed reaction phases have been limited to titanium oxides, including TiO [22,23], Ti<sub>2</sub>O [24] and Ti<sub>2</sub>O<sub>3</sub> [25], as well as copper-titanium oxides (Cu,Al)<sub>3</sub>Ti<sub>3</sub>O and Ti<sub>4</sub>Cu<sub>2</sub>O [26,27]. These compounds have demonstrated a noteworthy impact on improving wetting behaviour and bond strength. In addition, when brazing at higher temperatures for an extended duration, the reaction layer gets thicker, and the inhomogeneous reaction phase forms on the interface. It stops the active metal Ti activity, which in turn weakens the bond. Not all formations of intermetallic compounds strengthen the joint, but the intensity of the crystallinity in intermetallics influences the structural behaviour of the brazed ceramicmetal joint [28].

Ag-Cu-Ti alloys are preferred for their exceptional dependability as active brazing fillers. However, a notable drawback is that the relatively high liquidus temperature renders them unsuitable for brazing aluminium alloys with ceramics. A joining process has been proposed to establish a strong and reliable ceramic-metal joint, drawing on crucial insights from the aforementioned *in situ* study on active brazing. Importantly, this achievement is potentially viable at a low brazing temperature, i.e. operating at temperatures lower than the solidus temperature of the aluminium-based parent material [29].

The main topic of this research paper is the reactive mechanism at the ceramic-metal interface. It focuses on how titanium can improve the wetting behaviour of the ceramic surface through reaction layer formation. This was realized through additive manufacturing (AM) technology: the metallization of the alumina-faying surface with titanium by physical vapour deposition, followed by furnace brazing using conventional filler in a vacuum environment.

# II. Experimental

# 2.1. Brazing of alumina with Al-alloy

Polycrystalline alumina ( ${\rm Al_2O_3}$ , with 99.99% purity), Al6061-T6 aluminium alloy with dimensions of 15 mm  $\times$  10 mm  $\times$  8 mm and Al4047 filler (Morgan Advanced Ceramics in Hayward, CA) were the starting materials used for the experimental investigation. Table 1 displays the chemical composition of the commercially available Al6061-T6 alloy and Al4047 filler.

In a high-temperature vacuum furnace, the sandwiched metallized alumina ceramics was joined with an aluminium alloy and intermediate aluminium filler (Fig. 1). The plasma-assisted physical vapour deposition (PAPVD, M/s. Bangalore Plasmatek, India) technology was used to coat the Al<sub>2</sub>O<sub>3</sub> surface with Ti (their physical properties were compared in Table 2). The Al4047 aluminium filler alloy was used in the form of a 0.25 mm-thick strip. The filler material, selected in accordance with AWS A5.10, was made up of Al-12Si-0.3Cu and the brazing temperature was kept at 582 °C, which is the liquidus temperature recommended by the manufacturer. Cleaning the faying surface ultrasonically with acetone for 5 min ensured the removal of contaminants. The Al<sub>2</sub>O<sub>3</sub>-Al composite assembly was tightly held together with the right fixtures so that it was in

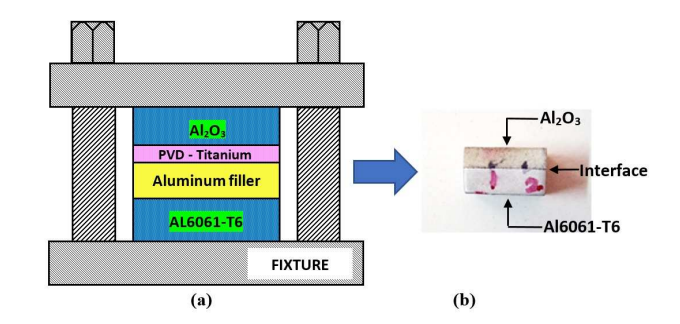


Figure 1. Schematic representation of sandwiched Ti metallized Al with Al6061-T6 alloy using Al filler (a) and vacuum brazed Ti metallized Al<sub>2</sub>O<sub>3</sub> with Al6061-T6 alloy (b)

Table 1. Chemical composition (wt.%) of commercially available aluminium base metal and brazing filler

Elements	Si	Fe	Cu	Mn	Mg	Zn	Cr	Ti	Others	Al
Aluminium 6061T6 alloy	0.7	0.6	0.30	0.05	0.9	0.20	0.25	0.10	0.05	Reminder
Aluminium 4047 filler	13	0.80	0.30	0.15	0.1	0.20	-	-	0.05	Reminder

Table 2. Melting point (T), thermal conductivity  $(\lambda)$ , density  $(\rho)$  and thermal expansion coefficient  $(\alpha)$  of Al6061-T6, Al4047 filler, alumina and pure titanium

Material	<i>T</i> [°C]	λ [W/m·K]	$\rho$ [g/cm <sup>3</sup> ]	$\alpha \ [\times 10^{-6}/K]$
Al6061-T6	582-652	167	2.70	23.6
A14047	577-613	121	2.68	21–23
$Al_2O_3$	2050	25-35	3.95-3.98	8.1-10.3
Pure Ti	1668	19.2	4.50	8.4

close contact with a joint clearance of 1.5 mm, which is suitable for capillary action. The brazing process entails subjecting the assembly to a liquidus temperature of the filler at a rate of 7 °C/min for 40 min. The brazing time of 40 min was selected according to the experimental study of the vacuum-brazed Al6061-T6 lap joint. It was shown [30] that after 30, 40 and 60 min of brazing at 582 °C with Al4047 filler, the brazed lap joint had an average tensile strength of about 31, 36 and 33 MPa, respectively. Following the brazing process, the brazed samples were cooled in a vacuum environment within the furnace. SiC abrasive with different grit sizes (500, 800 and 1200) was used to polish the brazed interface and diamond (0.25 µm) polishing paste was then used to make the face very smooth. Finally, the samples were cleansed using a lint-free cloth wetted with a mixture of hydrofluoric acid and distilled water.

# 2.2. Coating deposition by PAPVD

Plasma-assisted physical vapour deposition (PA-PVD) technology was implemented to coat the Al<sub>2</sub>O<sub>3</sub> faying surface with active metal titanium that was 5.93 µm thick on average in a high vacuum using a steered cathodic-arc titanium plasma source. A dense Ti layer was formed on the alumina substrate, size 50 mm × 25 mm, using the cathodic arc PVD method. During the pre-coating process, the ceramic surface was exposed to in situ glow discharge in argon plasma etching to improve its hydrophilicity, thereby easing optimal adhesion [31]. A vacuum arc with a 90 A current and a velocity range of 2 to 45 m/s was used to accelerate energetic Ti ions up to 150 eV and deposit them on a ceramic substrate for 3–7 min. The high-energy and stimulated momentum titanium atoms have effects on film growth by increasing the substrate temperature and materializing a denser, void-free film at a high flux ratio of bombarding ions to depositing atoms. Metallization of the alumina surface yields an enhancement in both the wetting performance and the strength of adhesion [32,33].

### 2.3. Heat treatment in vacuum furnace

In ceramic-metal brazing, vacuum atmosphere heating furnace plays a significant role in developing robust joints. Heat treatment in a vacuum atmosphere completely removes gases during the brazing and PVD coating processes. This is because it creates an atmosphere that makes it easier to remove residual gases from the assembly, impedes oxidation at high temperatures and ensures reliable brazed joints [34,35]. The use of Ti and Al, which are highly reactive metals, when processed in an uncontrolled atmosphere furnace at elevated temperatures, causes rapid oxidation. This oxidation, in turn, affects the ductility and strength of the brazed joints by forming an oxide layer at the interface [36]. Ti and Al are metals with a negative redox potential and a stronger attraction to oxygen. This means that titanium compounds can be in different oxidation states, and also +3, which is the most common for aluminium compounds [37]. The vacuum shields the deposition process against gaseous contamination by having a substantial mean-free path between atom-ion collisions and the reduced boiling point of the deposited film. Integrating vacuum technology with PVD and brazing processes improves the ceramic surface's wetting behaviour and even achieves reliable bond strength [20].

#### 2.4. Characterization

Scanning electron microscope, SEM, with an energy-dispersive X-ray, EDX was used to characterize the elemental composition at the brazed interface. X-ray diffraction, XRD technique enabled characterizing the reaction phase peaks corresponding to the JCPDS (Joint Committee on Powder Diffraction Standards) database.

## III. Results and discussion

## 3.1. Interfacial microstructure characterization

The vacuum-brazed Al<sub>2</sub>O<sub>3</sub>-Al interface was analysed by SEM (Fig. 2). The brazing seam consists of five phases (indicated in Fig. 2 with points A, B, C, D and E) and its energy dispersive X-ray spectrometry (EDX) analysis is shown in Table 3. The phases A and B were deduced to be Ti-O-Al. Titanium has greater solubility in oxygen in comparison to aluminium. This resulted in significant wetting and spreading characteristics on the joining surface due to a chemical reaction. With 41.12 wt.% Al, 58.43 wt.% Si and 0.41 wt.% Cu, the phase C is an Al-Si eutectic structure that is high in Si. The phase D is an Al-Cu eutectic structure with 73.64 wt.% Al, 1.35 wt.% Si and 24.8 wt.% Cu. The brazing seam is flawless, which might increase element diffusion and interfacial reactivity, which made the joint stronger. The significantly lower liquidus of the Al4047

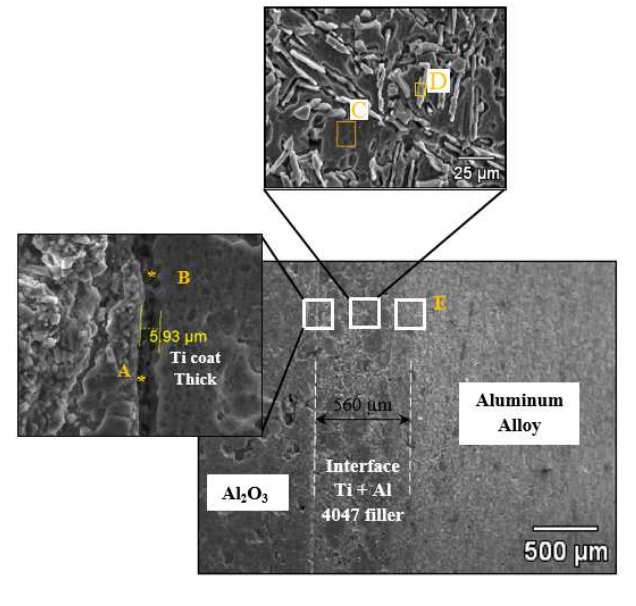


Figure 2. SEM micrograph of a cross-section view of the  $Al_2O_3/PVD$  titanium/Al4047/Al6061-T6 alloy joint brazed at 582 °C for 40 min in  $1\times10^{-5}$  mbar vacuum

Location Composition [wt.%]							Possible reaction		
Location	Al	Ti	Fe	Si	Cu	О	phases		
A	30.71	38.90	0	0	0	30.39	Ti-O and Ti-Al		
В	0	98.70	0	0	0	1.30	Ti-rich		
C	41.12	0	0.04	58.43	0.41	0	Si-Al, Si-rich		
D	73.64	0.14	0.07	1.35	24.8	0	Al-Ti-Cu		
E	88.24	0.05	0	10.49	1.22	0	Al-Cu-Si, Al (s,s)		

Table 3. EDS results of different phases determined from Fig. 2

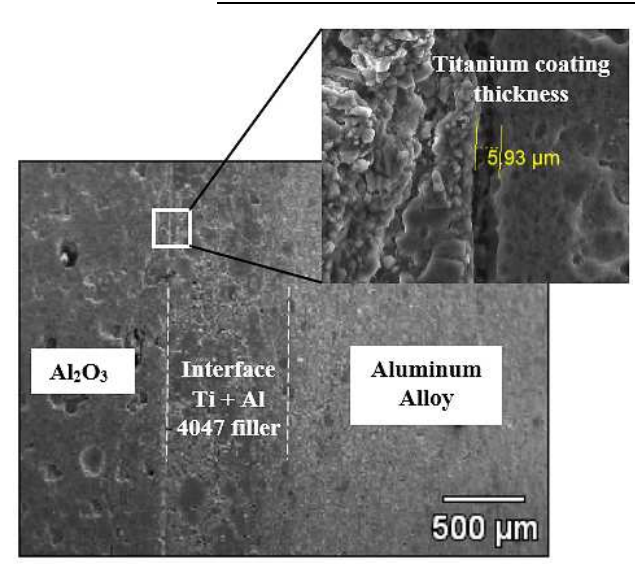


Figure 3. SEM micrograph of a cross-section view of the  $Al_2O_3/PVD$  titanium/Al4047/Al6061-T6 alloy joint brazed at 582 °C for 40 min in  $1\times10^{-5}$  mbar vacuum

filler metal facilitates the formation of a robust joint in the Al<sub>2</sub>O<sub>3</sub>/Al alloy brazing. This elucidates its capacity to wet and disperse effectively within the joint clearance of the joining materials that were investigated.

This research article is focused predominantly on the interaction at the  $Al_2O_3$ -Ti interface in the brazed  $Al_2O_3$ /Ti/Al4047/Al alloy system (Fig. 3). The interface is decoded based on the reactive mechanism at the  $Al_2O_3$ -Ti interfaces with the main question how does titanium influence the bonding characteristics of the alumina-aluminium composites.

The SEM micrographs with EDX mapping (Figs. 4, 5 and 6) show that the Ti-O and Ti-Al phases were found where the titanium meets the alumina, and the Ti-Al-Si compound formed where the titanium meets the filler alloy. Rajendran et al. [28] documented the observation of double intermetallic thick layers on the alumina side derived from a brazed Al<sub>2</sub>O<sub>3</sub>/Cu system using Ag-Cu-Sn-Zr-Ti metallic filler. However, a reaction layer of 0.5–1 µm thickness was identified with Ti-O and Ti-Al phases. At the alumina-titanium interface, TiO<sub>2</sub> and Ti<sub>3</sub>Al were confirmed by XRD analysis, as shown in Fig. 5. The XRD pattern of the Al<sub>2</sub>O<sub>3</sub>/Al alloy interface shows various diffraction peaks. At the Al<sub>2</sub>O<sub>3</sub>/Ti interface, the intermetallic compound peaks were confirmed to be TiO<sub>2</sub> with anatase properties that matched the JCPDS card number #21-1272 (crystal system: hexagonal; space lattice: body-centered; space

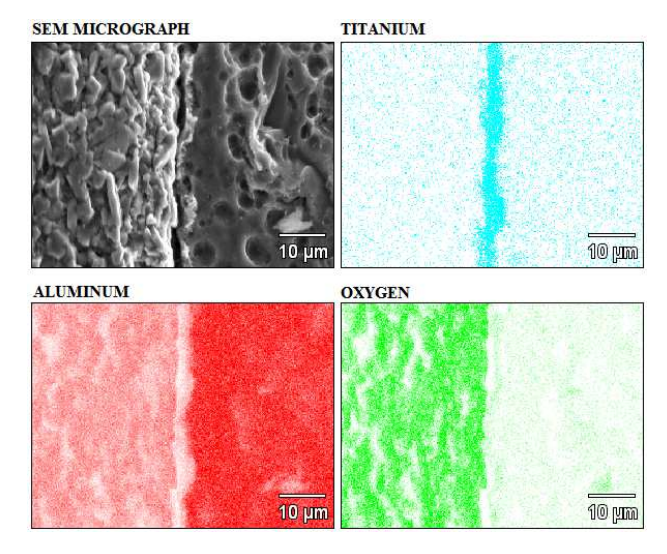


Figure 4.  $Al_2O_3/Ti$  interface: SEM microstructure and elemental distribution on the  $Al_2O_3/PVD$  Titanium/Al4047 filler joint brazed at 582  $^{\circ}C$  for 40 min

group: I41/amd; space group number: 141;  $a=b=3.785\,\text{Å}$ ,  $c=9.513\,\text{Å}$ ;  $\alpha=\beta=\gamma=90^\circ$ ). In addition, the Ti<sub>3</sub>Al peaks were also found using the JCPDS card number #14-0451 (crystal system: hexagonal; space lattice: primitive; space group: P63/mmc; space group number: 194;  $a=b=5.77\,\text{Å}$ ,  $c=4.62\,\text{Å}$ ;  $\alpha=\beta=90^\circ$ , and  $\gamma=120^\circ$ ).

The formation of TiO<sub>2</sub> is caused by the dissolution of Ti atoms which tends to react rigorously with the oxygen atoms released at the Al<sub>2</sub>O<sub>3</sub> ceramic faying surface [38]. At higher temperatures, the reaction is spontaneous for the negative Gibbs free energy ( $\Delta G_f$ ) of formation, defined by the combination of subsiding energy and increasing entropy. The  $\Delta G_f$  is a comparative measure of the stability of a metallic compound with respect to the pure metal element, which is a function of temperature and pressure. Based on the formation energy ( $\Delta G_f$ ), TiO<sub>2</sub> and Ti<sub>3</sub>Al are usually extremely stable intermetallic compounds, as validated by their considerable negative  $\Delta G_f$  of -940.4 + 0.181T kJ/mol for  $TiO_2$  and -29.6 + 0.007T kJ/mol for  $Ti_3A1$  [39,40]. Titanium is more reactive to oxygen than aluminium. Besides, Ti has a superior attraction to silicon in combination with aluminium and copper in the molten filler alloy [26,41]. As shown in Fig. 5, the microstructural elemental mapping analysis reveals that the reaction layer includes Ti-O-Al compounds that also exist on the interface. The research outcomes support the perspective that the thicker the interfacial reaction layer formation

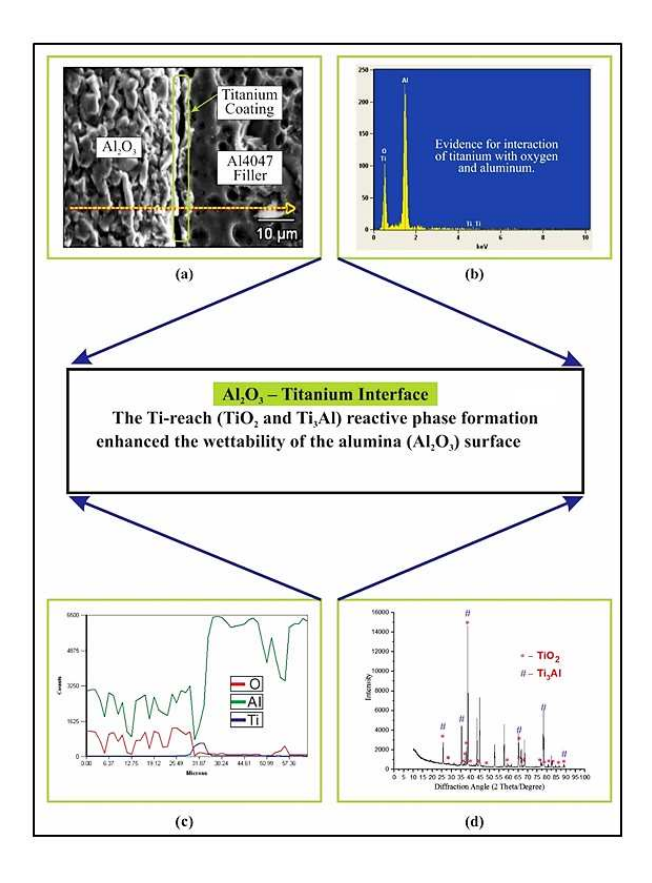


Figure 5. Al<sub>2</sub>O<sub>3</sub>/Ti interface: SEM micrograph with elemental mapping analysis and EDS line scan analysis (a, b, c) and XRD pattern confirming presence of TiO<sub>2</sub> and Ti<sub>3</sub>Al phases (d)

over the increased brazing period, the less Ti activity with the  ${\rm Al_2O_3}$  surface due to the lower solubility of  ${\rm TiO_2}$  [38,42]. Titanium stimulation in the interfacial microstructural formation has a greater impact on improving the wetting and spreading behaviour of the  ${\rm Al_2O_3}$  substrate [43].

During the extended 40-minute processing period, the formation of Ti-rich interfacial region at the  $Al_2O_3$  surface intensified (Fig. 6) as there was reduced interfacial free energy that led to better wetting effect through

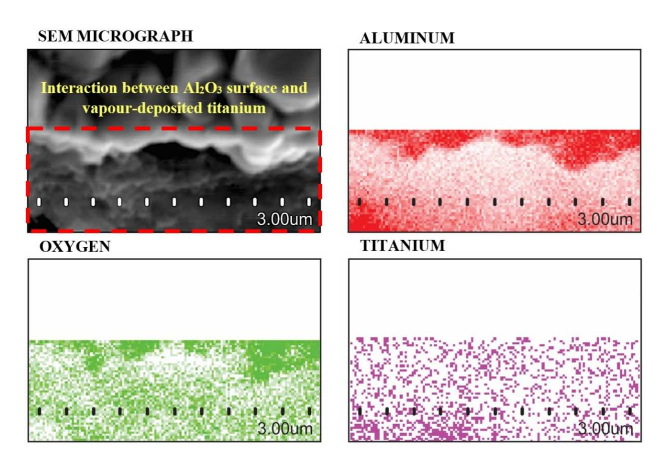


Figure 6. SEM micrograph, coupled with elemental distribution observation, elucidates the existence of titanium adsorption onto the alumina surface

chemical reactions. This led to a proportional reduction in the degree of crystallinity and ductility of the titanium coating [44]. In addition, the SEM micrograph (Fig. 6) shows significant titanium enrichment at the Al surface, as Ti atom reduces Al<sub>2</sub>O<sub>3</sub> due to the superior Ti-O bond energy relative to the Al-O bond energy [45,46]. This explains why the TiO<sub>2</sub> phase is present in greater amounts than the Ti<sub>3</sub>Al phase, as shown in the XRD pattern (Fig. 5d). At a higher brazing temperature for the prolonged brazing time, Ti atoms dissolve further into the interfacial reaction layer near the alumina substrate, reacting with Al and O, as well as through the interface with the Al-Si-Cu filler alloy, thereby forming a thicker reaction layer [47]. Consequently, the interfacial microstructure of the alumina/titanium and titanium/filler alloy systems will change. This was also demonstrated in the Al<sub>2</sub>O<sub>3</sub>/Al<sub>2</sub>O<sub>3</sub> brazed joint with the observation of reaction phases Ni<sub>2</sub>Ti<sub>4</sub>O and AlNi<sub>2</sub>Ti formed on the NiTi/Al<sub>2</sub>O<sub>3</sub> interface [48,49]. The Ni<sub>2</sub>Ti<sub>4</sub>O reaction layer grows thicker and the columnar AlNi<sub>2</sub>Ti phase becomes coarser with the extended brazing time, leading to a decline in joint strength [48,49]. The spreading of the molten filler took place on the reaction layer adjacent to the Al<sub>2</sub>O<sub>3</sub> substrate. Meanwhile, the thicker the formed layer at the interface, the lower the Ti activity across the ceramic-metal interface, which in turn weakens the mechanical properties [50].

An investigation of the time-dependent microstructural growth at the Al<sub>2</sub>O<sub>3</sub>/TiAl interface during brazing at 880 °C by means of a silver-based active filler has provided constructive insights into the bonding mechanism and the effect of brazing time on the joint characteristics, which varied from 1 to 30 min [19,51]. AlCu<sub>2</sub>Ti phase formation intensified with brazing time. The intermetallic Ti<sub>3</sub>(Cu,Al)<sub>3</sub>O reaction layer thickened from 1.5 to 3 µm over a period of 30 min of brazing. At first, chemical reactions controlled the intermetallic growth kinetics. As the reaction layer got thicker, these reactions prevented titanium from diffusing into the ceramics. It was observed that a thicker Al-CuTi reaction layer adjoins the metal filler and TiAl substrate. The observation emphasizes that processing at higher brazing temperatures for a longer period deepens the dispersion of molten filler within the TiAl alloy. This results in the formation of a thicker Ti<sub>3</sub>(Cu,Al)<sub>3</sub>O layer with a blocky AlCu<sub>2</sub>Ti compound. Investigation of the Al<sub>2</sub>O<sub>3</sub>/TiAl joint probed the influence of brazing time over interfacial microstructure formation and shear strength brazed at 900 °C [52-54]. The presence of fragmented AlCu<sub>2</sub>Ti in the intermetallic (Cu,Al)<sub>3</sub>Ti<sub>3</sub>O reaction layer had a significant effect on joint integrity. When it comes to determining the physical properties of (Ti-6Al-4V/AISI 321), (ZrO<sub>2</sub>/SS316), (YAG/Kovar), (AlMgB<sub>14</sub>-TiB<sub>2</sub>/SS304), (Ti-6Al-4V/AISI 321), (Al<sub>2</sub>O<sub>3</sub>/Ni-Ti) and (SiO<sub>2f</sub>/SiO<sub>2</sub> composite) joints, the study stressed how important the brazing duration is. Because of the extended brazing time, a thick and brittle (TiO and Cu<sub>2</sub>Ti<sub>4</sub>O), (Fe<sub>2</sub>Ti and

Ni<sub>3</sub>Ti), (Cu(Ti,Al)ss and TiB whisker), (CuTi<sub>2</sub>, CuTi, FeTi, Fe<sub>22</sub>Zn<sub>78</sub> and TiZn<sub>3</sub>), (Ni<sub>2</sub>Ti<sub>4</sub>O and AlNi<sub>2</sub>Ti) and (Cu<sub>x</sub>Ti<sub>6-x</sub>O) intermetallic phases were formed, which significantly reduced the bond strength of the composite materials.

## 3.2. Fracture characterization

The 2%-rule in brazing is a significant directive for non-destructive evaluation by radiography. X-ray inspection procedure could not identify the defects in the brazed joints when the joint clearance is less than 2% of the thickness of the base materials brazed together [55,56]. Figure 7 presents a radiograph of a brazed joint satisfying the 2%-rule. It exemplifies the brazed specimen of Al<sub>2</sub>O<sub>3</sub> ceramics with Al alloy, both of 3 mm thickness, with a joint clearance of 1.5 mm, through which X-rays are transmitted for better defect sensitivity analysis. It is a clear and concise description of the surface morphology of a lap joint, presenting observations on the uniformity and smoothness of the brazed seam established through sufficient brazing alloy flow and proper joint clearances in a vacuum atmosphere. However, obvious breakage of the alumina substrate (tiny portion) on the top corner of the brazed specimen was observed from radiography. The evolution of cracks and delamination can be reduced considerably or even prevented with the controlled heating rate (7 °C/min) to minimize thermal stresses. Customization of the brazing temperature and holding time ensures optimal metal filler flow. Moreover, regulation of the cooling rate helps avert prompt cooling and the use of suitable fixtures supports minimizing distortion and stresses. The significance of the aforementioned measures is exemplified in Fig. 7, where neither micropores, incomplete fusion and voids, nor cracks (longitudinal or transverse) across the brazed lap joint are identified as defects.

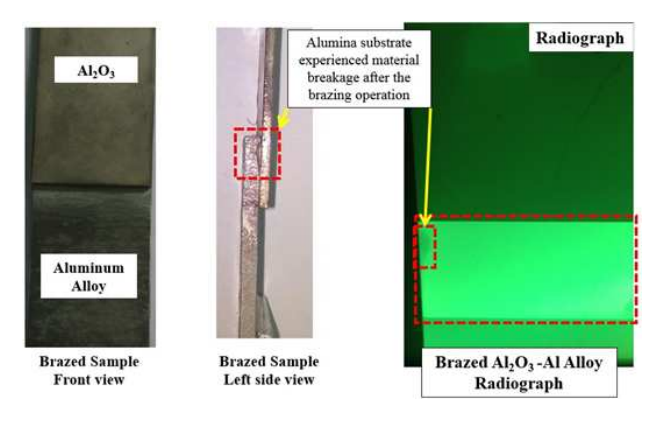


Figure 7. X-ray inspection of the brazed Al<sub>2</sub>O<sub>3</sub>-Al alloy

The overall characterizations could reveal beneficial elements, including: i) a detailed look at how Ti affects the wetting behaviour of the Al surface using SEM (Figs. 3 and 6), ii) a study of the Ti-rich intermetallic compound development and its structure using XRD method adjoined to the  $Al_2O_3$  surface with Ti deposition (Fig. 5) and iii) a radiograph that checked the degree





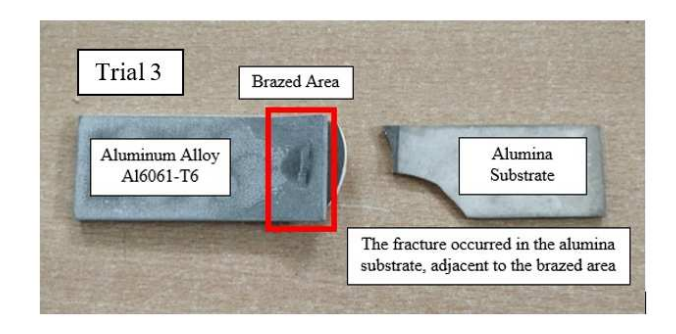


Figure 8. Brazed  $Al_2O_3$ -Al joint with Ti coating: Fractured surface in the  $Al_2O_3$  side of the joint brazed at 582  $^{\circ}$ C for 40 min in a vacuum atmosphere

of joint quality of the brazed part to examine any flaws (Fig. 7). In order to reinforce the foregoing, an attempt was made to determine how much load the brazed specimen could withstand. The samples after tensile testing of the brazed Al<sub>2</sub>O<sub>2</sub>/Al lap joints are shown in Fig. 8. It could be concluded that the inclusion of Ti layer had an influence on the tensile properties of the brazed joints. The tensile strength of the brazed joints with and without Ti PVD coating is given in Table 4; meanwhile, the elongation also had the same change rule, as shown in Fig. 9. The Ti-coated Al<sub>2</sub>O<sub>3</sub>/Al brazed joint had a tensile strength of 29 MPa. All the trials fractures (1, 2 and 3) fracture happened in the alumina substrate away from the brazed zone due to its brittle nature as shown in Fig. 8 and Table 4. The titanium coating layer enhanced the wetting and bonding behaviour between alumina and aluminium filler. The fracture morphology of the alumina substrate in the Ti-coated Al<sub>2</sub>O<sub>3</sub>/Al joint displays a brittle fracture, typically transgranular and intergranular fracturing of the ceramic substrate. For the brazed Al<sub>2</sub>O<sub>3</sub>/Al joint without titanium PVD coating, the alumina peeled off the aluminium base material during the initial stage of the tensile testing, with no indication of elongation in the stress-strain curve. This was debonding, not fracture, due to the poor wetting behaviour of the Al4047 filler intermetallics on the Al<sub>2</sub>O<sub>3</sub> surface, as shown in Fig. 10. This proved that the titanium interlayer and the brazing parameters used were effective and yielded rewarding results.

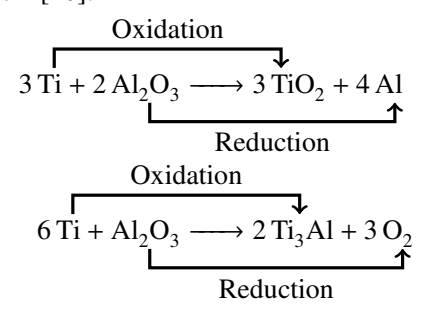
Spec	cimen details	Remarks				
Brazed Al <sub>2</sub> O <sub>3</sub> /Al	Specimen 1	In all the trials (1, 2, and 3), fracture happened in the Al <sub>2</sub> O <sub>3</sub> base				
joint with Ti PVD	Trial 1 - $\sigma_J$ = 25.18 MPa	material away from the brazed zone due to its brittle nature. The				
coating (Fig. 8)	Trial 2 - $\sigma_J$ = 26.04 MPa	Ti coating layer enhanced the wetting and bonding behaviour				
	Trial 3 - $\sigma_J = 29.44 \text{MPa}$	between Al <sub>2</sub> O <sub>3</sub> and Al filler				
Al <sub>2</sub> O <sub>3</sub> /Al joint		Testing Failed due to debonding, not fracture. Al <sub>2</sub> O <sub>3</sub> peeled off				
without Ti PVD coating (Fig. 9)	Specimen 2	the Al base material. The Al filler did not bond to the Al <sub>2</sub> O <sub>3</sub> surface because it lacks active metal elements, such as Ti, which are necessary to improve the wetting behaviour of the ceramics.				
30 25 Trial 1:	25.18 MPa 25 EN 20 V 15 V 1	Trial 2: 26.04 MPa  25  25  20  20  21  21  22  23  24  20  25  25  25  26  27  28  28  20  28  21  25				

Table 4. Al<sub>2</sub>O<sub>3</sub>/Al joint strength (σ) brazed at 582 °C for 40 min in a vacuum atmosphere

Figure 9. Stress-strain curves of the brazed Al<sub>2</sub>O<sub>3</sub>/Al joint with Ti coating: a) trial 1, b) trial 2 and c) trial 3

## 3.3. Al<sub>2</sub>O<sub>3</sub>-Ti interfacial reaction mechanism

The wetting behaviour of the reaction layer formed along the ceramic-metal interface at the triple line aids in the spreading of molten active brazes across the titanium-metallized alumina surface [19]. Titanium accelerates the spreading rate of the  $Al_2O_3$  surface by forming a reaction compound at the interface. It is observed from the  $Al_2O_3/Ti$  interface that the Ti atoms have a greater affinity for oxygen. The interaction of Ti atoms with released oxygen and Al on the  $Al_2O_3$  substrate develops intermetallic compounds [41].  $TiO_2$  and  $Ti_3Al$  reaction compounds promote the formation of the reaction layer in the vicinity of the triple line. The following equations elaborate on the potential reaction mechanism [40]:



The idea explores the -2 anion in Al<sub>2</sub>O<sub>3</sub> being displaced by the +2 Ti cation in combination with an oxidation-reduction reaction, which emanates from the chemical bonding at the ceramic-metal interface. The electron affinity of Ti is greater compared to that of Al and O [19]. The atomic radii of the elements correlate with their affinity to form chemical bonds. When the number of protons decreases, the nucleus gets less positively charged. The attraction force between the nucleus and electrons in the outermost shell decreases, as does the positive charge. The electrons slack in relation to the nucleus, which is greatly attracted by the higher-affinity

oxygen, resulting in a decrease in electron affinity [57]. The titanium inclusion decreases the interfacial tension with the increase in the work of adhesion on the ceramic surface at a high level of wetting for the set brazing temperature [58].

The degree of crystallinity of the titanium-rich reaction compounds was assessed from XRD pattern using the peak deconvolution method [59]. Peak width broadening and crystallite size have had inverse variations following the Scherrer equation [60]. A wider peak indicates smaller crystallite sizes for the ductile intermetallics. The crystallinity of the reaction products was greatly disturbed by lattice imperfections and displaced atomic arrangements processed at higher temperatures [61]. The narrow diffractions observed in the peaks of TiO<sub>2</sub> and Ti<sub>3</sub>Al phases (Fig. 5d) correspond to the substantial crystallinity of the titanium-reacted phases. The crystallinity increases with oxygen replacement. The intermetallic crystallinity decreases with an increase in the substitution of oxygen and aluminium in the titanium lattice. This is evident from the progressively reducing peak intensities.

To comprehend the  $Al_2O_3/Ti$  interface, it is important to determine whether the reaction layer forms at high temperatures or at the solidification stage during the brazing process. In addition, it is important to understand how much does the formation of reaction compounds impact reactive wetting. Based on the brazed CuAg-Ti/alumina system observations, which were examined at  $900\,^{\circ}C$ , featuring a heating duration extending from 3 to  $600\,\text{min}$ , the thickness of the interfacial reaction layer grows in a parabolic form as a function of time, and its increase is proportional to the brazing time [19]. Similarly, a reduction in the coating thickness of the pure titanium was documented concurrently with the increasing extent of intermetallic formation on the  $Al_2O_3$  surface during a 40-minute processing period.

At the experimental temperature, a dense reaction layer formed on the Al<sub>2</sub>O<sub>3</sub> surface for a prolonged brazing time because Ti interacted strongly with the Al and O. Creation of Ti-Al-O reaction composites at the Al<sub>2</sub>O<sub>3</sub>/Ti interface while heating at 582 °C stops titanium from dissolving any further. This maintains the titanium concentration below the necessary threshold for a reaction with the alumina surface [54].

Brazing alumina and aluminium alloy together produced a thin, ductile Ti-O-Al intermetallic compound that was about 0.5–1 µm thick. This happened at 582 °C for 40 min in a vacuum. The thickness of the intermetallic compound developed by this method was less than the layer thickness found in the active brazing experiment with the CuAg-Ti/alumina system [5]. Interlayers containing vapour-deposited titanium and an aluminium-silver-copper alloy filler inhibited the formation of a thicker, more brittle intermetallic compound between the Al<sub>2</sub>O<sub>3</sub> and Al alloys. To achieve optimal results, it is important to use brazing conditions for a brief period at high temperatures (above the liquidus temperature) that avoid thicker reaction compound formation at the interface. The primary objective of the proposed methodology was to improve the mechanical integrity of ceramic-metal interconnections by stabilizing the ductility of both Ti and Al fillers. In a successful first attempt, the research initiative into the joining method demonstrated profound efficacy in bridging the ductile aluminium filler with the brittle alumina ceramics using a titanium interlayer for composite assemblies in sensor feedthroughs.

# IV. Conclusions

Ceramic-to-metal joining ( $Al_2O_3/Al6061$ -T6 aluminium alloy) was achieved through additive manufacturing (AM) technology integrating plasma-assisted physical vapour deposition (PAPVD) to metallize the  $Al_2O_3$  surface with Ti, which was brazed using the eutectic Al4047 filler at 582 °C for 40 min in a vacuum atmosphere.

An intense titanium electron beam of  $150\,\mathrm{eV}$  generated at  $90\,\mathrm{A}$  vacuum arc current, produces a dense Ti coating with no voids. As the focus of the research is on the  $\mathrm{Al_2O_3/Ti}$  interface, the influence of Ti on habituating wetting through chemical reactions was investigated by analytical techniques.

It was concluded that the high-affinity titanium activates the reaction at the  $Al_2O_3$  surface at high temperatures, which is the cause of reliable bonding at the interface. The microstructure grows with Ti-rich phases through the redox reaction process. The interfacial reaction layer thickness of 0.5–1  $\mu m$ , adjacent to the  $Al_2O_3$  surface, was identified as  $TiO_2$  and  $Ti_3Al$  phases, which contribute significantly to enhancing the wetting activity of the ceramic surface.

Chemically stable  $Al_2O_3$  underwent reduction by Ti, a process substantiated by the thermodynamic reaction at the interface. Ti-coated  $Al_2O_3/Al$  joint fractured

in the ceramic substrate away from the brazed area at 29 MPa, exhibiting characteristic brittle, transgranular and intergranular fractures. The brazing method effectively averts the development of a thick, brittle intermetallic compound layer adjoining  $Al_2O_3$  and Al through the strategic integration of an eutectic aluminium filler and plasma-assisted physical vapour deposition of titanium.

**Acknowledgement:** The authors gratefully acknowledge the support of the DST-FIST, Government of India and the Department of Ceramic Technology, Anna University, India.

# References

- Y.-K. Sun, S.-Y. Chang, L.-C. Tsao, T.-H. Chuang, G.-Z. Zhang, C.-Y. Yeh, "Effects of adding active elements to aluminum-based filler alloys on the bonding of 6061 aluminum alloy and alumina", *Appl. Sci.*, 11 [21] (2021) 10440.
- Y.-T. Wang, Y.-H. Cheng, C.-C. Lin, K.-L. Lin, "Direct bonding of aluminum to alumina using a nickel interlayer for power electronics applications", *Results Mater.*, 6 (2020) 100093.
- 3. X.-S. Ning, Y. Lin, W. Xu, R. Peng, H. Zhou, K. Chen, "Development of a directly bonded aluminum/alumina power electronic substrate", *Mater. Sci. Eng. B*, **99** [1-3] (2003) 479–482.
- C.-Y. Lin, W.-H. Tuan, "Direct bonding of aluminum to alumina for thermal dissipation purposes", *Int. J. Appl. Ceram. Technol.*, 13 (2015) 170–176.
- S. Stalin, K. Kalaichelvan, "Ceramic-metal interface: Insitu microstructural characterization aid vacuum brazing additive manufacturing technology", pp. 235–251 in Advances in Additive Manufacturing Artificial Intelligence, Nature-Inspired, and Biomanufacturing. Ed. R.K.M.A.H. Ajay Kumar, Elsevier, 2022.
- H. Bian, X. Song, S. Hu, Y. Lei, Y. Jiao, S. Duan, J. Feng, W. Long, "Microstructure evolution and mechanical properties of titanium/alumina brazed joints for medical implants", *Metals*, 9 [6] (2019) 644.
- 7. J.H. Schulman, "Brain control and sensing of artificial limbs", pp. 275–291 in *Implantable Neural Prostheses 1*, Eds. E. Greenbaum, D. Zhou, Springer, 2009.
- K. Ely, Y. Zhou, "Microjoining in medical components and devices", pp. 691–717 in *Series in Welding and other Join*ing *Technologies, Microjoining and Nanojoining*. Ed. Y. Zhou, Woodhead, 2008.
- 9. G. Sala, "Advanced metal-ceramic joining techniques for orthopaedic applications", pp. 407–448 in *Joining and Assembly of Medical Materials and Devices*. Eds., Y. Zhou, M.D. Breyen, Woodhead Publishing, 2013.
- G. Jiang, D.D. Zhou, "Technology advances and challenges in hermetic packaging for implantable medical devices", pp. 27–61 in *Implantable Neural Prostheses 2*. Eds. D. Zhou, E. Greenbaum, Springer, 2010.
- 11. D.-I.H. Wampers, "Alumina systems GmbH", Alumina systems GmbH, 1970. [Online]. Available: https://alumina.systems/en/. [Accessed November 2023]
- 12. Y. Lei, H. Bian, W. Fu, X. Song, J. Feng, W. Long, H. Niu, "Evaluation of biomedical Ti/ZrO<sub>2</sub> joint brazed with pure Au filler: Microstructure and mechanical properties",

- Metals, 10 [4] (2020) 526.
- W.D. Kaplan, D. Brandon, *Joining Processes: An Introduction*, 1<sup>st</sup> Ed., Wiley, 1997.
- 14. X. Chen, J. Yan, S. Ren, J. Wei, Q. Wang, "Ultrasonic-assisted brazing of SiC ceramic to Ti-6Al-4V alloy using a novel AlSnSiZnMg filler metal", *Mater. Lett.*, **105** (2013) 120–123.
- 15. B. Zhou, J. Wang, K. Feng, Y. Cai, S. Chen, "Effect of brazing parameters on the microstructure and properties of SiC ceramic joint with Zr-Cu filler metal", *Crystals*, **10** [2] (2020) 93.
- G. Wang, Y. Yang, P. Wu, D. Shu, D. Zhu, C. Tan, W. Cao, "Effect of brazing temperature on microstructure and mechanical properties of TiAl/ZrB<sub>2</sub> joint brazed with Cu-TiZrNi filler", *J. Manufact. Process.*, 46 (2019) 170–176.
- W.-W. Li, B. Chen, L.-M. Cao, W. Liu, H.-P. Xiong, Y.-Y. Cheng, "Joining of C<sub>f</sub>/SiBCN composite with CuPd-V filler alloy", *J. Mater. Sci. Technol.*, 34 [9] (2018) 1652–1659.
- D.M. Jacobson, G. Humpston, *Principles of Brazing*, 1<sup>st</sup>
   Ed., Ohio, ASM International, 2005, pp. 221–249.
- 19. R. Voytovych, F. Robaut, N. Eustathopoulos, "The relation between wetting and interfacial chemistry in the CuAgTi/alumina system", *Acta Mater.*, **54** [8] (2006) 2205–2214.
- S. Grosso, L. Latu-Romain, G. Berthomé, G. Renou, T. Le Coz, M. Mantel, "Titanium and titanium nitride thin films grown by dc reactive magnetron sputtering Physical Vapor Deposition in a continuous mode on stainless steel wires: Chemical, morphological and structural investigations", Surf. Coat. Technol., 324 (2017) 318–327.
- T.I. Selinder, E. Coronel, E. Wallin, U. Helmersso, "α-alumina coatings on WC/Co substrates by physical vapor deposition", 27 [2] (2009) 507–512.
- 22. D. Janičkovič, P. Šebo, P. Duhaj, P. Švec, "The rapidly quenched Ag-Cu-Ti ribbons for active joining of ceramics", *Mater. Sci. Eng. A*, **304-306** (2001) 569–573.
- S. Mandal, A.K. Ray, A.K. Ray, "Correlation between the mechanical properties and the microstructural behaviour of Al<sub>2</sub>O<sub>3</sub>-(Ag-Cu-Ti) brazed joints", *Mater. Sci. Eng. A*, 383 [2] (2004) 235–244.
- K.-L. Lin, M. Singh, R. Asthana, "Interfacial characterization of alumina-to-alumina joints fabricated using silver-copper-titanium interlayers", *Mater. Charact.*, 90 (2014) 40–51.
- 25. Q. Lin, K. Tan, L. Wang, R. Sui, "Wetting of YSZ by molten Sn-8Zr, Sn-4Zr-4Ti, and Sn-8Ti alloys at 800–900 °C", *Ceram. Int.*, **48** [1] (2022) 373–380.
- 26. L. Wang, A. K. Tieu, Q. Zhu, J. Chen, J. Cheng, J. Yang, B. Kosasih, "Achieving the excellent self-lubricity and low wear of TiAl intermetallics through the addition of copper coated graphite", *Composites Part B: Eng.*, **198** (2020) 108223.
- Y. Liang, J. Kong, K. Dong, X. Song, X. Liu, R. Zhu, "Microstructure evolution and mechanical properties of vacuum brazed ZrO<sub>2</sub>/Ti-6Al-4V joint utilizing a low-melting-point amorphous filler metal", *Vacuum*, 192 (2021) 110456.
- 28. S. Rajendran, S. Hwang, J. Jung, "Active brazing of alumina and copper with multicomponent Ag-Cu-Sn-Zr-Ti filler", *Metals*, **11** [3] (2021) 509.
- 29. S. Stalin, K. Kalaichelvan, "Ceramic-metal interface: the influence of titanium on the microstructure of vacuum

- brazed alumina-aluminum alloy", pp. 129 in *The 56<sup>th</sup> Annual Meeting of the Israel Society for Microscopy*, May 23<sup>rd</sup>, 2023, Binyanei Hauma ICC, Jerusalem, Israel.
- 30. K. Kalaichelvan, *Development and Formability studies on Hybrid Metallic Sandwich Composites for thermal Protection in Hypersonic Aircraft Skins*, Aeronautics Research and Development Board (AR&DB), 2019.
- J.T. Gudmundsson, A. Anders, A. von Keudell, "Foundations of physical vapor deposition with plasma assistance", *Plasma Sources Sci. Technol.*, 31 (2022) 083001.
- 32. H.R. Prabhakara, V.L. Tanna, "Trapping of dust and dust acoustic waves in laboratory plasmas", *Phys. Plasma.*, **3** (1996) 3176–3181.
- 33. D.M. Mattox, *Handbook of Physical Vapor Deposition* (PVD) Processing, Elsevier, 2010.
- T. Romano, G. Pikurs, A. Ratkus, T. Torims, N. Delerue, M. Vretenar, L. Stepien, E. López, M. Vedani, "Metal additive manufacturing for particle accelerator applications", *Phys. Rev. Accel. Beams*, 27 (2024) 054801.
- 35. M. Boretius, "Ceramic-metal compounds produced by means of vacuum brazing", *Liste-mann Technology AG*, 2019. [Online]. Available: https://info.listemann.com/en/blog/ceramic-metal-compounds-produced-by-means-of-vacuum-brazing.
- D.K. Creber, J. Ball, D.J. Field, "A mechanistic study of aluminum vacuum brazing", SAE Transactions, 96 (1987) 648–655.
- 37. C.R. Goldsmith, "Aluminum and gallium complexes as homogeneous catalysts for reduction/oxidation reactions", *Coordin. Chem. Rev.*, **337** (2018) 209–224, 2018.
- 38. X. Chenglai, L. Ning, Y. Jiazhen, C. Yongtong, "Effects of Ti activity on mechanical properties and microstructures of Al<sub>2</sub>O<sub>3</sub>/Ag-Cu-Ti/Fe-Ni-Co brazed joints", *Rare Metal Mater. Eng.*, **47** [4] (2018) 1031–1036.
- 39. E. Kashkarov, M. Krinitcyn, A. Dyussambayev, A. Pirozhkov, M. Koptsev, "Structure and properties of porous Ti<sub>3</sub>AlC<sub>2</sub>-doped Al<sub>2</sub>O<sub>3</sub> composites obtained by slip casting method for membrane application", *Materials*, **16** [4] (2023) 1537.
- 40. C.C. Chen, "Phase equilibria at Ti-Al interface under low oxygen pressure", *Atlas J. Mater. Sci.*, **1** [1] (2014) 1–11.
- 41. W.D. Kaplan, D. Chatain, P. Wynblatt, W. Craig Carter, "A review of wetting versus adsorption, complexions, and related phenomena: the rosetta stone of wetting", *J. Mater. Sci.*, **48** (2013) 5681–5717.
- 42. M. Ali, K.M. Knowles, P.M. Mallinson, J.A. Fernie, "Microstructural evolution and characterisation of interfacial phases in Al<sub>2</sub>O<sub>3</sub>/Ag-Cu-Ti/Al<sub>2</sub>O<sub>3</sub> braze joints", *Acta Mater.*, **96** (2015) 143–158.
- Y. Li, C. Wang, X. Li, L. Zhang, P. Pan, M. Lei, "Brazing YAG ceramic to Kovar alloy with Ag-Cu-Ti filler alloy: Wettability, microstructure and mechanical properties", *Vacuum*, 213 (2023) 112093.
- 44. J.C. Oliveira, A. Manaia, A. Cavaleiro, M.T. Vieira, "Structure, hardness and thermal stability of Ti(Al,N) coatings", *Surf. Coat. Technol.*, **201** [7] (2006) 4073–4077.
- M. Shen, M. Wang, Q. Wang, J. Tian, L. Zhang, L. Wang, J. Shi, "A Ti-OH bond breaking route for creating oxygen vacancy in titania towards efficient CO<sub>2</sub> photoreduction", *Chem. Eng. J.*, 425 (2021) 131513.
- 46. G. Li, C. Zhao, Q. Yu, F. Yang, J. Chen, "Revealing Al-O/Al-F reaction dynamic effects on the combustion of aluminum nanoparticles in oxygen/fluorine containing envi-

- ronments: A reactive molecular dynamics study meshing together experimental validation", *Defence Technol.*, **34** (2024) 313–327.
- F. Moszner, G. Mata-Osoro, M. Chiodi, J. Janczak-Rusch, G. Blugan, J. Kuebler, "Mechanical behavior of SiC joints brazed using an active Ag-Cu-In-Ti braze at elevated temperatures", *Int. J. Appl. Ceram. Technol.*, 14 [4] (2017) 703–711.
- 48. Q. Zhang, Y. Lu, J. Wang, K. Zheng, W. Xue, H. Yang, "Enhanced bonding of Al<sub>2</sub>O<sub>3</sub>/Al<sub>2</sub>O<sub>3</sub> joints brazed by Ni<sub>50</sub>Ti<sub>50</sub> master alloy interlayer", *Vacuum*, **185** (2021) 110000.
- Y. Lu, M. Zhu, Q. Zhang, T. Hu, J. Wang, K. Zheng, "Microstructure evolution and bonding strength of the Al<sub>2</sub>O<sub>3</sub>/Al<sub>2</sub>O<sub>3</sub> interface brazed via Ni-Ti intermetallic phases", J. Eur. Ceram. Soc., 40 [4] (2020) 1496–1504.
- W.C. Lee, O.Y. Kwon, C.S. Kang, "Microstructural characterization of interfacial reaction products between alumina and braze alloy", *J. Mater. Sci.*, 30 (1995) 1679–1688.
- Z. Yang, J. Lin, Y. Wang, D. Wang, "Characterization of microstructure and mechanical properties of Al<sub>2</sub>O<sub>3</sub>/TiAl joints vacuum-brazed with Ag-Cu-Ti + W composite filler", *Vacuum*, 143 (2017) 294–302.
- 52. X.P. Liu, L.X. Zhang, Z. Sun, J.C. Feng, "Microstructure and mechanical properties of transparent alumina and TiAl alloy joints brazed using Ag-Cu-Ti filler metal", *Vacuum*, **151** (2018) 80–89.
- G. Niu, D. Wang, Z. Yang, Y. Wang, "Microstructure and mechanical properties of Al<sub>2</sub>O<sub>3</sub> ceramic and TiAl alloy joints brazed with Ag-Cu-Ti filler metal", *Ceram. Int.*, 42

- [6] (2016) 6924-6934.
- X. Dai, J. Cao, J. Liu, S. Su, J. Feng, "Effect of holding time on microstructure and mechanical properties of ZrO<sub>2</sub>/TiAl joints brazed by Ag-Cu filler metal", *Mater. Design*, 87 (2015) 53–59.
- 55. J. Kar, S. Kumar Dinda, G. Gopal Roy, S. Kumar Ro, P. Srirangam, "X-ray tomography study on porosity in electron beam welded dissimilar copper-304SS joints", *Vac-uum*, **149** (2018) 200–206.
- 56. D. Kay, "X-Ray inspection of brazed joints", *Kay Brazing*, Kay & Associates, [Online]. Available: https://www.kaybrazing.com/brazing-articles/1000906-x-ray-inspection-of-brazed-joints.html. [Accessed November 2023].
- 57. J. Cao, X. Si, W. Li, X. Song, J. Feng, "Reactive air brazing of YSZ-electrolyte and Al<sub>2</sub>O<sub>3</sub>-substrate for gas sensor sealing: Interfacial microstructure and mechanical properties", *Int. J. Hydrog. Energy*, **42** [15] (2017) 10683–10694.
- 58. M. Nicholas, *Joining of Ceramics*, Springer, New York, 1990.
- 59. A.S. Goikhman, V.M. Irklei, O.S. Vavrinyuk, V.I. Pirogov, "X-ray diffraction determination of the degree of crystallinity of cellulose using a computer", *Fibre Chem.*, **24** (1992) 80–85.
- D.G. Chukhchin, A.V. Malkov, I.V. Tyshkunova, L.V. Mayer, E.V. Novozhilov, "Diffractometric method for determining the degree of crystallinity of materials", *Crystallogr. Rep.*, 61 (2016) 371–375.
- 61. J. Langford, A. Wilson, "Scherrer after sixty years: A survey and some new results in the determination of crystallite size", *J. Appl. Cryst.*, **11** (1978) 102–113.